Electronic Supplementary Material (ESI) for Journal of Materials Chemistry B.

Supporting Information

Regulation of multifunctional mesoporous core-shell nanoparticles with luminescence and magnetic properties for biomedical applications

Xiaoqing Hu, Mingliang Wang, Fei Miao, Jingwei Ma, Hebai Shen, Nengqin Jia*

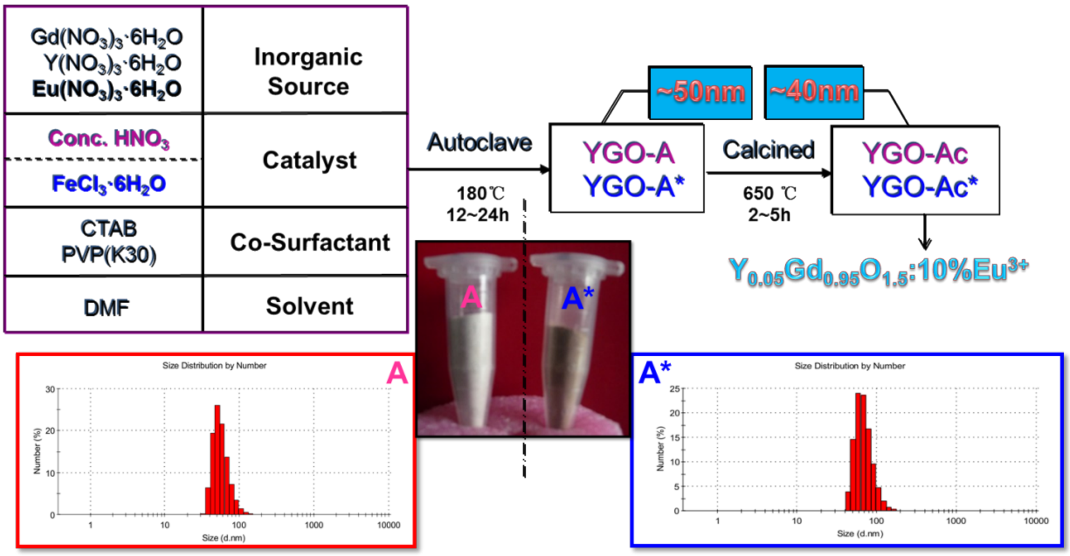

Figure S1. Flow chart of solvothermal synthetic procedures for $(Y,Gd)_2O_3:Eu^{3+}$ NPs. The inset at the bottom: DLS size distribution (in ethanol) of YGO-A NPs (left) and YGO-A* NPs (right).

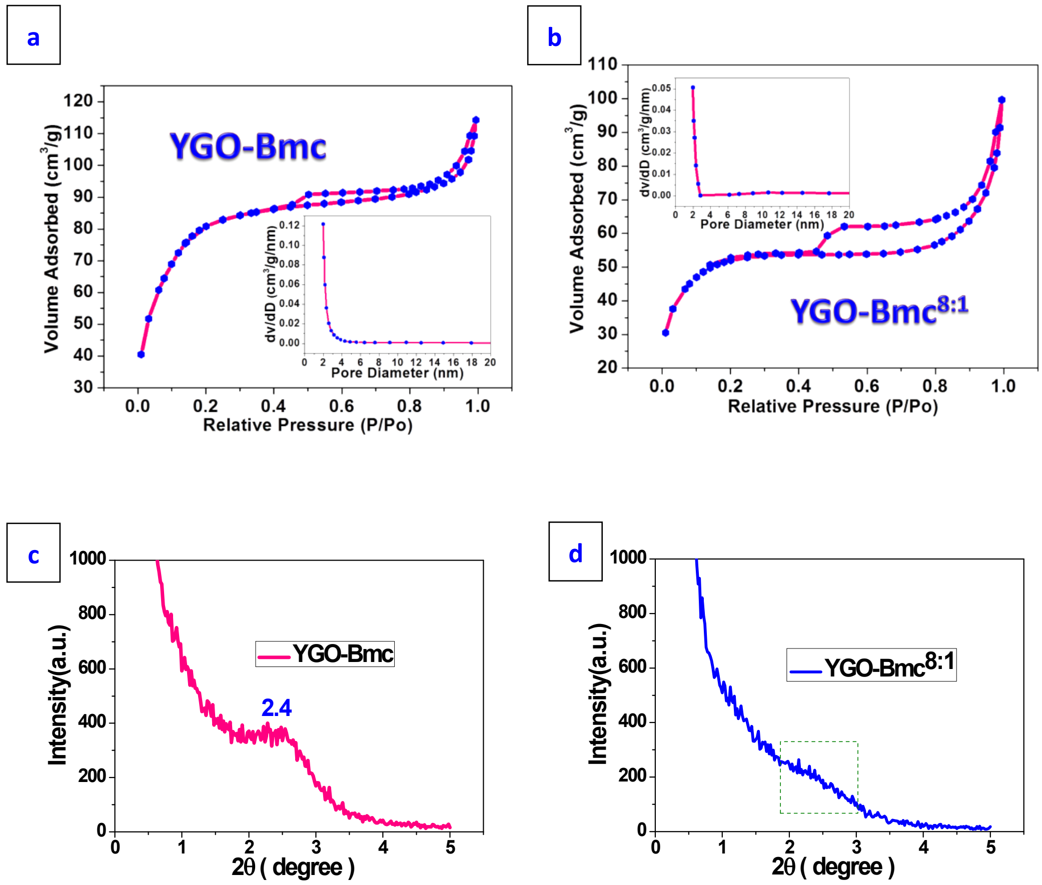

Figure S2. N_2 adsorption/desorption isotherms and mesopore size distribution curves (the inset) of (a) YGO-Bmc NPs, (b) YGO-Bmc$^{8:1}$ NPs; low-angle XRD patterns of (c) YGO-Bmc NPs, (d) YGO-Bmc$^{8:1}$ NPs.

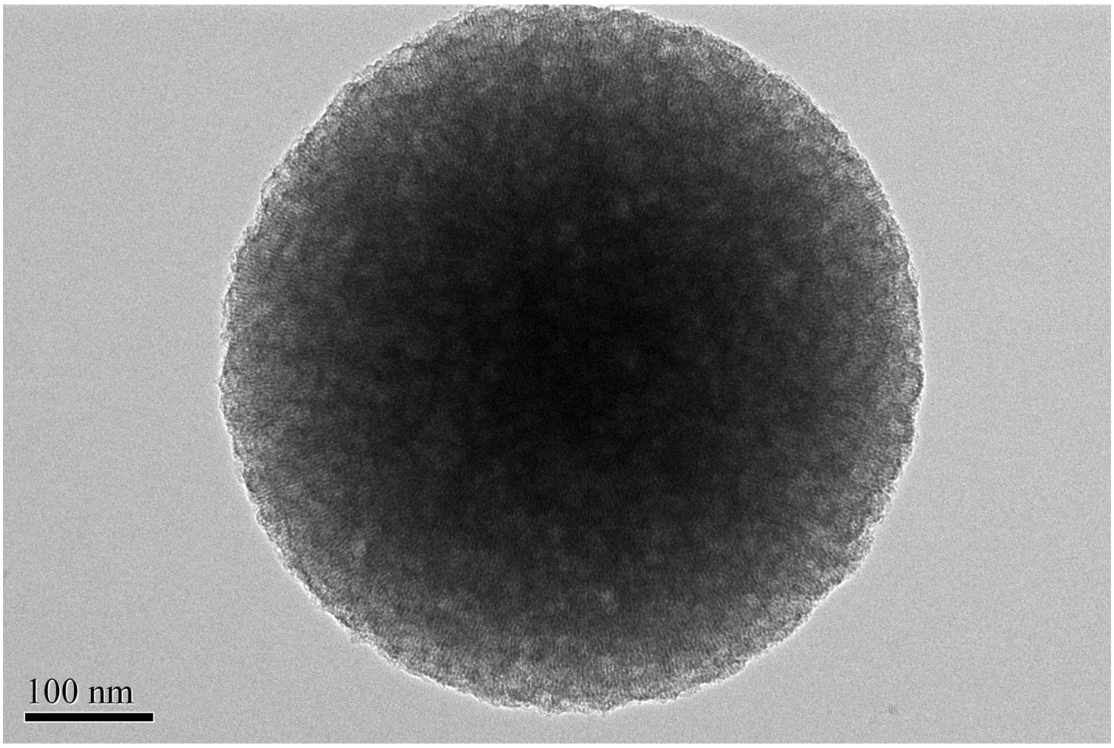

Figure S3. TEM image of $mSiO_2$.

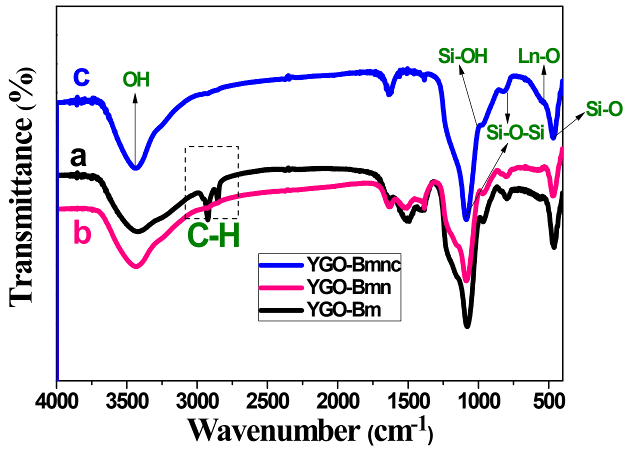

Figure S4. The FT-IR spectra of (a) YGO-Bm NPs, (b) YGO-Bmn NPs, (c) YGO-Bmnc NPs. Contrary to YGO-Bm NPs, the bands in the region 2800~3000 cm^{-1} which attributed to the vibrations of $-CH_3$, $-CH_2$ of CTAB templates disappeared for YGO-Bmn NPs, suggesting that the CTAB templates are eradicated completely after NH_4NO_3/EtOH extraction. For YGO-Bmnc NPs, the new characteristic vibration of Ln-O bond in 543 cm^{-1} turns up, demonstrating that the amorphous $Ln(OH)_3$ completely dehydrated and transformed into Ln_2O_3 after calcination.

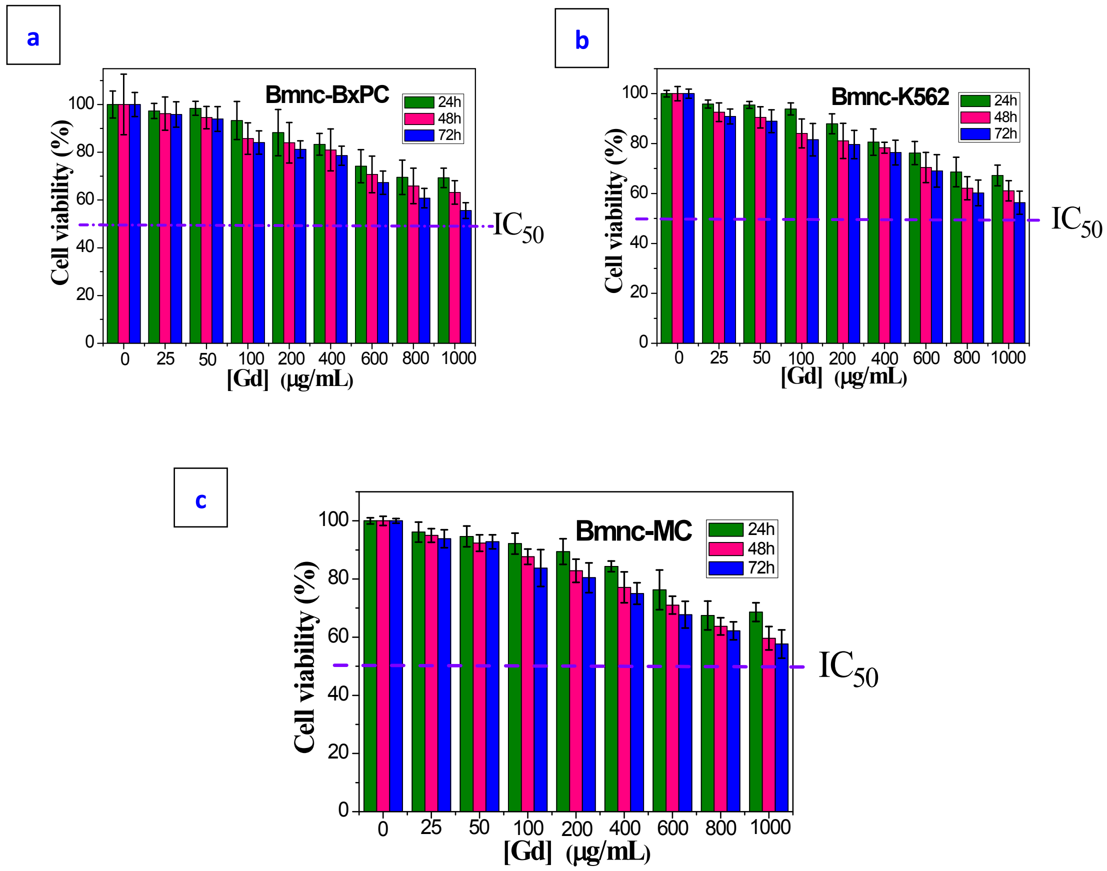

Figure S5. In vitro cytotoxicity of YGO-Bmnc NPs against BxPC-3, K562 and MC cells after 24 h, 48 h and 72h incubation.